Clinical, Radiographic, and Morphometric Risk Factors for Adjacent and Remote Vertebral Compression Fractures Over a Minimum Follow-up of 4 Years After Percutaneous Vertebroplasty for Osteoporotic Vertebral Compression Fractures: Novel Three-dimensional Voxel-Based Morphometric Analysis

Hong-Jae Lee[1], Jinah Park[2], Il-Woo Lee[1], Jin-seok Yi[1], Taeho Kim[2]

■ OBJECTIVE: **This study aimed to analyze the risk factors for secondary new vertebral compression fractures (SNVCFs) after percutaneous vertebroplasty (PVP) for osteoporotic vertebral compression fractures.**

■ METHODS: **We evaluated the association of SNVCFs (adjacent vertebral compression fractures [AVCFs] and remote vertebral compression fractures) with clinical, radiographic, and PVP procedure-related morphologic parameters based on the data collected from 402 patients over a minimum follow-up of 4 years after PVP. Procedure-related morphologic parameters were assessed using a three-dimensional voxel-based analysis. Univariate and multivariate regression analyses were conducted.**

■ RESULTS: **On univariate analysis, bone mineral density (BMD), preoperative compression ratio, preoperative sagittal index (SI), and intradiscal bone cement leakage were significantly associated with SNVCF and AVCF ($P < 0.05$), whereas only BMD and preoperative SI were significantly associated with remote vertebral compression fracture ($P < 0.05$). A large ratio of bone cement volume to vertebral body volume and skewed bone cement distribution along the inferior-to-superior axis were especially significant risk factors for AVCF ($P = 0.027$ and $P = 0.029$, respectively). On multivariate analysis, BMD was significantly associated with SNVCF ($P = 0.041$), whereas upper adjacent intradiscal bone cement leakage was significantly associated with AVCF ($P = 0.003$).**

■ CONCLUSIONS: **Low BMD, high preoperative compression ratio, and high preoperative SI may be predictive factors for SNVCFs. In particular, to prevent AVCF, the injected bone cement should be distributed both evenly and symmetrically along the inferior-to-superior axis and the relative bone cement volume should not be excessive. Bone cement should be injected carefully to avoid upper adjacent intradiscal leakage. Prompt BMD correction is important to prevent SNVCF.**

INTRODUCTION

The superiority of percutaneous vertebroplasty (PVP) over conservative treatment in the management of osteoporotic vertebral compression fracture (OVCF) has not been confirmed based on prospective randomized controlled

Key words
- Bone mineral density
- Osteoporosis
- Percutaneous vertebroplasty
- Risk factor
- Vertebral compression fracture
- Voxel

Abbreviations and Acronyms
ADV: Adjacent disc volume
AVCF: Adjacent vertebral compression fracture
BCV: Bone cement volume
BMD: Bone mineral density
BMI: Body mass index
CR: Compression ratio
CT: Computed tomography
KA: Kyphotic angle
LIBCV: Leaked intradiscal bone cement volume
MRI: Magnetic resonance imaging
OVCF: Osteoporotic vertebral compression fracture
PVP: Percutaneous vertebroplasty
RVCF: Remote vertebral compression fracture
SI: Sagittal index
SNVCF: Secondary new vertebral compression fracture
VBV: Vertebral body volume

From the [1]Department of Neurosurgery, The Catholic University of Korea, College of Medicine, Daejeon St. Mary's Hospital Seoul; and [2]School of Computing, Korea Advanced Institute of Science and Technology, Daejeon, Korea

To whom correspondence should be addressed: Hong-Jae Lee, M.D, Ph.D. [E-mail: kosailee73@gmail.com]

Hong-Jae Lee and Jinah Park contributed equally to the work and hence should be considered as co-first authors.

Citation: World Neurosurg. (2019) 125:e146-e157.
https://doi.org/10.1016/j.wneu.2019.01.020

*Journal homepage: **www.journals.elsevier.com/world-neurosurgery***

*Available online: **www.sciencedirect.com***

comparative trials.[1-3] However, PVP has become a widely used treatment for painful OVCF because this procedure is minimally invasive, relatively safe, and highly effective at improving pain and pain-related disabilities caused by OVCF.[1-5] Although many studies have reported the usefulness, relatively low risk, and increased performance of PVP procedures, many PVP-related complications have been described, including nerve injury, vascular injury, hematoma, hemothorax, bone cement leakage, emboli, infection, and secondary new vertebral compression fracture (SNVCF).[6,7] SNVCF represents the most problematic complication and thus has been the topic of many medical research studies because of its clinical importance and high incidence, which was reported to be 12%–52%.[8-11] Many risk factors of SNVCF have been reported, including body mass index (BMI),[12] preoperative bone mineral density (BMD),[13-16] number of OVCFs,[2,17,18] segmental kyphotic angle (KA),[19,20] sagittal index (SI),[12,21] preoperative compression ratio (CR),[15] thoracolumbar junctional fracture,[22] intradiscal bone cement leakage,[16,22-25] injected bone cement volume (BCV),[11,26,27] and bone cement distribution in the vertebral body.[28,29] However, many issues related to SNVCF remain under debate because of the methodological limitations of many previous studies. Many studies have reported conflicting results regarding the risk factors for SNVCF, including BMI, number of OVCFs, KA, SI, preoperative CR, thoracolumbar junctional fracture, and intradiscal bone cement leakage, because of different cohort size and follow-up periods.[13,19] In the present study, we used data from a large cohort with a long follow-up. Specifically, many previous clinical studies of BCV have evaluated the injected BCV based on medical record data, which may have been inaccurate. Other previous clinical studies about bone cement distribution used bone cement location data based on two-dimensional images,[13] which may have been inaccurate and cannot reflect the symmetry of the bone cement distribution in 3 dimensions. On the contrary, three-dimensional voxel-based morphometry allows for an accurate understanding and precise measurement of structural changes throughout the PVP-treated vertebral body.[30,31] Therefore, in the present study, we used three-dimensional voxel-based morphometry for analyses of BCV and bone cement distribution to clarify the risk factors of SNVCF after PVP for OVCF.

METHODS

Patients

We retrospectively evaluated the records of consecutive patients who underwent PVP for OVCF between January 2011 and December 2013. The study was conducted in conformance with the approval of the institutional review board of our hospital. The patients provided informed consent for undergoing the procedures. Because this was a retrospective study using anonymized data, the requirement for informed consent was waived. The study included only patients with a minimum follow-up of 4 years who were evaluated using radiographs, BMD measurements, and magnetic resonance imaging (MRI) for the diagnosis of OVCF. The use of antiosteoporosis drugs was not included as a risk factor for SNVCF, but the study included only those patients who took antiosteoporotic drugs, including bisphosphonate or selective estrogen receptor modulators after OVCF diagnosis. During 2011–2013, bisphosphonate and selective estrogen receptor modulators (selective estrogen receptor modulators) were routinely used after diagnosis of osteoporosis, and parathyroid hormone analogue or receptor activator κ B ligand were not used at our hospital. For all enrolled patients, acute OVCF was confirmed via MRI (Magnetom Verio 3T [Siemens, Berlin, Germany]) and osteoporosis was confirmed based on a T score <-2.5 on BMD evaluation. Patients with pathologic fractures, a history of previous spinal surgery (PVP, simple decompression surgery, or spinal fusion surgery), spinal infection or systemic diseases, including vitamin D deficiency, and previous paresis inducing osteoporosis, were excluded. Of the 661 patients evaluated, the follow-up loss rate was 4%, and 402 patients met the inclusion criteria and were analyzed.

Study Design

The patients were stratified according to the number of affected vertebral levels (single level vs. multiple level). Simple regression analysis was used to evaluate the association between SNVCF and the number of OVCFs in 79 patients with multiple-level OVCFs. To remove the bias that could be caused by the interaction between the initial number of OVCFs and SNVCF incidence, further analyses of the association of SNVCF, adjacent vertebral compression fracture (AVCF), and remote vertebral compression fracture (RVCF) with potential risk factors were conducted in the group of 323 patients with single-level OVCF. Such factors included BMI, vertebroplasty technique, preoperative segmental KA, SI, and CR, thoracolumbar junction fractures, intradiscal bone cement leakage, ratio of BCV to vertebral body volume (VBV), bone cement distribution in the fractured vertebral body, and ratio of leaked intradiscal BCV (LIBCV) to the adjacent disc volume (ADV). In the present study, VBV, BCV, and bone cement distribution in the fractured vertebral body, as well as LIBCV and ADV, were determined via three-dimensional voxel-based analysis of postoperative computed tomography (CT) or MRI data. Because postoperative CT or MRI was not routinely performed after PVP, the three-dimensional voxel-based analysis included only data of patients who underwent CT or MRI for different reasons within 6 months postoperatively (182 of 402 patients included in the study).

Vertebroplasty Procedure

Three different spine surgeons performed the procedures. All procedures were performed with the patient in the prone position, after minimal sedation was induced by intravenous administration of opioids. Vital signs and arterial oxygen saturation levels were monitored using pulse oximetry during the course of the surgery. A 13-gauge bone marrow biopsy needle (Angiotech Pharmaceuticals Inc., Vancouver, Canada) was introduced into the vertebral body via the bilateral transpedicular or unilateral extrapedicular approach under C-arm fluoroscopic guidance (Siemens, Munich, Germany). After contrast-enhanced venography (Visipaque [GE Healthcare, Cork, Ireland]), bone cement composed of polymethyl methacrylate powder and barium sulfate powder (Elmdown Ltd, London, United Kingdom) was injected under C-arm fluoroscopic guidance. Postoperative radiographs were obtained after 6 hours of bed rest to identify any complications.

Data Collection

Patient characteristics including age, sex, BMI, medical history (diabetes mellitus, hypertension, smoking, spinal surgery, vitamin

D deficiency, and previous paresis), and duration of follow-up were obtained from the medical records. Information regarding the specific vertebroplasty technique (bilateral transpedicular approach or unilateral extrapedicular approach) and the time interval between PVP and SNVCF was also obtained from the medical records. Preoperative segmental KA, SI, and vertebral CR representing the degree of kyphotic deformity caused by OVCF were measured on the radiographic images.[12] Segmental KA was measured using the most reliable modified Cobb method and the SI was obtained by subtracting the normal sagittal angle from the kyphotic deformity at the fractured vertebra (Figure 1).[12,21,32,33] CR was measured using the following equation: (anterior height of lower vertebra + anterior height of upper vertebra)/2—anterior height of fractured vertebra/(anterior height of lower vertebra + anterior height of upper vertebra/2). Preoperative BMD, number of OVCFs, thoracolumbar junction fractures, and intradiscal bone cement leakage were assessed on the radiographic images. One experienced spine surgeon measured and recorded the radiographic data. Postoperative radiographs were obtained at regular outpatient visits at 1 month, 2 months, 4 months, and 12 months. Patients treated with PVP, regardless of regular visits, were instructed to visit the outpatient clinic in the event of a clinical or neurologic impairment. Physical examination, radiography, and MRI were performed whenever the patient had back pain, and SNVCF was diagnosed based on MRI findings.

Three-Dimensional Voxel-Based Analysis

Procedure-specific parameters including the fractured VBV, injected BCV, bone cement distribution in the vertebral body, LIBCV, and ADV were assessed using a three-dimensional voxel-based analysis, which was first attempted in spinal surgery, because it precisely measures structural changes in cemented vertebra after PVP for OVCF.[30,31] The voxel-based analysis consists of 2 steps: 1) segmentation of vertebral body and cemented areas of interest and 2) cement distribution analysis, as described in the following sections.

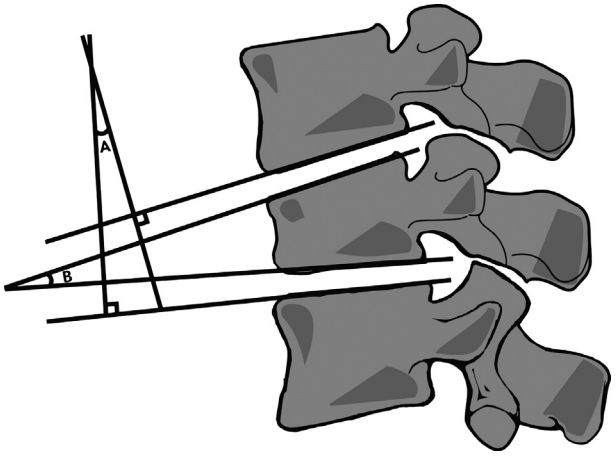

Figure 1. Measurement of segmental kyphotic angle and sagittal index. (**A**) Segmental kyphotic angle was measured using the modified Cobb method and the angle between the lower end plate of the adjacent vertebral body above the treated level and the upper end plate of the adjacent vertebral body below the treated level was defined. (**B**) Kyphotic deformity at the fractured vertebra: the sagittal index was obtained by subtracting the normal sagittal angle from the kyphotic deformity at the fractured vertebra. The normal sagittal angle was defined as a 5° kyphosis for thoracic vertebrae, neutral alignment for the twelfth thoracic and first lumbar vertebrae, and that of a 10° lordosis for the lumbar vertebrae.

Segmentation. We established a volumetric measurement environment based on an open-source medical image analysis software library, MITK (Medical Imaging Interaction Toolkit [German Cancer Research Center, Heidelberg, Germany]), in which an image segmentation plug-in was reserved for separating the desired region (vertebral body or bone cement) from the original CT or MRI data. A custom plug-in module was also developed to facilitate consistent interpretation of the distribution of bone cement compared within the treated vertebral body. Segmentation of the vertebral body was performed by first drawing representative contours of the PVP-treated vertebral body on a few selected slices of the axial CT or MRI scans and then applying two-dimensional interpolation to obtain the contour of the corresponding region on the remaining slices (Figure 2A—C). The image region corresponding to the injected bone cement was segmented by first applying an automatic thresholding technique based on the image intensity and then refining the result by eliminating any misclassified regions (Figure 2D—F). The image segmentation process was conducted by 3 researchers associated with medical engineering projects (for 8 years, 1.5 years, and 1 year, respectively). The voxel (volume element), which is a basic unit of three-dimensional CT or MRI volumetric image data, represents a unit volume comprising the pixel on two-dimensional CT or MRI together with the slice thickness. Voxels were labeled according to whether they belonged to the image region representing the vertebral body or to the region representing the bone cement. The physical position of each voxel was computed using the information from the image header. The volume of the vertebral body and that of the injected bone cement were measured as the volumes defined by the sum of voxels labeled as belonging to the vertebral body or injected cement regions, respectively.

Three-Dimensional Model for Analysis. To analyze bone cement distribution within the vertebral body, a three-dimensional mesh (surface) model of polyhedral vertebral body was constructed using a marching cube algorithm applied to the segmented image of the fractured vertebral body (Figure 2G and H). The three-dimensional mesh model was used to calculate the center of the fractured vertebral body and to define local axes of reference.[34] Three local axes were defined (inferior-to-superior, left-to-right, and anterior-to-posterior) using a model-based feature detection algorithm that approximates the orientation of 2 neighboring end plates, left, right, anterior, and posterior ends of a vertebral body from a three-dimensional mesh model of a polyhedral fractured vertebral body (Figure 2I and J).[34] With respect to the local frame of reference, the position of the voxels labeled as bone cement was vectorized to measure the distance and direction of each voxel from the center of mass of the vertebral body and thus determine the distribution of bone cement with reference to each of the 3 local axes. We visualized the bone cement—augmented area within the vertebra

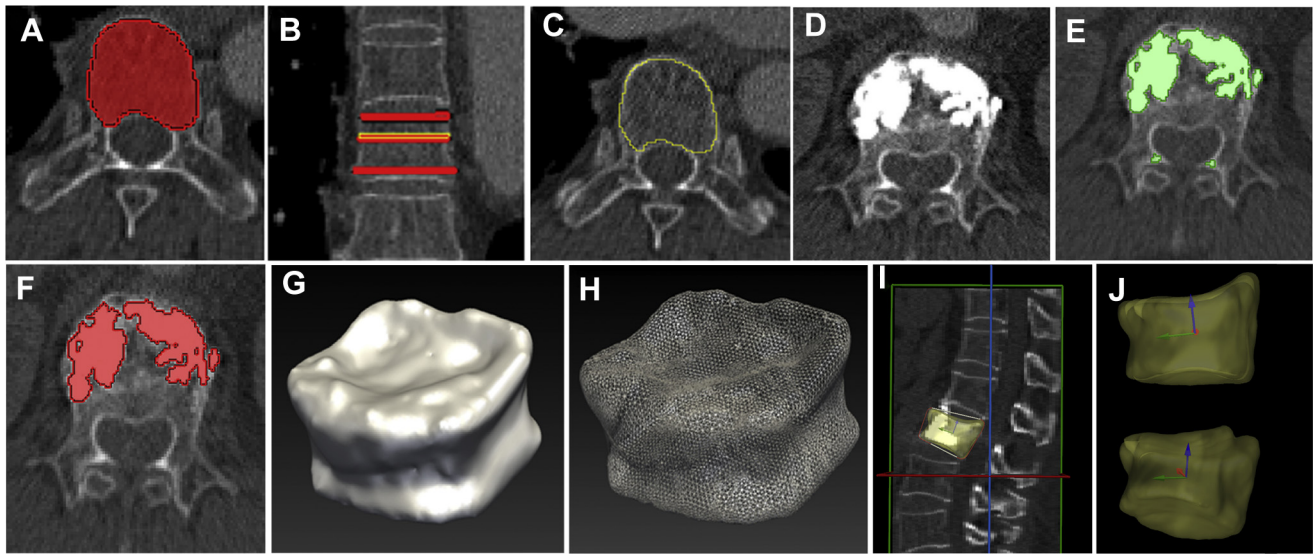

Figure 2. Segmentation and three-dimensional mesh model of the treated vertebra. (**A**) Two-dimensional segmentation results on a selected axial slice. (**B**) Selected slices shown on a computed tomography coronal scan. (**C**) Interpolated contour in a neighboring slice. (**D**) Target bone cement on a computed tomography axial scan. (**E**) Automatic region selection using a thresholding algorithm. (**F**) Refined segmentation result reflecting the bone cement. (**G**) Reconstructed three-dimensional vertebral body model. (**H**) Mesh representation of the model. (**I**) Reconstructed vertebral body model with its local axes overlaid on a computed tomography sagittal scan. (**J**) Three-dimensional visualization of the reconstructed model with its center and 3 axes (left-to-right axis, *red*; posterior-to-anterior axis, *green*; inferior-to-superior axis, *blue*) of the local reference frame.

and plotted the voxel distribution along each axis (Figure 3) to comprehensively understand the three-dimensional spatial distribution of the bone cement and quantify its symmetry aspects. Cement distribution analyses were performed using histograms of the positions of the vectorized voxels along each axis (inferior-to-superior axis, left-to-right axis, and anterior-to-posterior axis), for which we computed the mean, median, mode, standard deviation, skewness, kurtosis, minimum and maximum bone cement, and vertebral body voxel values.[35] The values of skewness and kurtosis showed how evenly and symmetrically the bone cement was injected into the vertebral body.[35] The spatial aspect of the bone cement distribution was also evaluated based on the minimum and maximum values of the bone cement voxels relative to the boundaries of the vertebral body. Bone cement was considered well distributed within the vertebral body if the range (from maximum to minimum) of bone cement voxels covered the center of the vertebral body and, simultaneously, the following findings held true: (maximum value−minimum value of bone cement voxels)/(maximum value−minimum value of vertebral body voxels) $\geq$0.5. Furthermore, bone cement was considered evenly and symmetrically distributed in the vertebral body if the |skewness| was below the median |skewness| noted in the evaluated population and kurtosis was <0.[35] The median |skewness| values serving as cutoffs for defining evenness and symmetry were set at 0.1903 for the inferior-to-superior axis, 0.1576 for the left-to-right axis, and 0.15335 for the anterior-to-posterior axis. Thus, the bone cement distribution in the vertebral body was evaluated using 4 criteria: 1) |skewness| < median |skewness|; 2) kurtosis <0; 3) range of bone cement voxel covering the center of the vertebral body; and 4) (maximum value−minimum value of bone cement voxels)/(maximum value−minimum value of vertebral body voxels) $\geq$0.5.[35]

Statistical Analysis

P values were calculated using the χ^2 test or Fisher exact test for categorical variables, and the *t* test or Wilcoxon rank-sum test for continuous variables. In this study, each risk factor was assessed for its association with SNVCF, AVCF, and RVCF using both univariate and multivariate analyses. Odds ratios were calculated using logistic regression. A Kaplan-Meier survival curve was used to evaluate the fracture-free rate and the time interval from PVP to AVCF and then RVCF. A *P* value of <0.05 was considered to indicate statistical significance. The Department of Biostatistics of our research center was consulted regarding the design of the statistical analyses for this study. All statistical analyses were performed using SAS Enterprise Guide 4 (SAS Institute Inc., Cary, North Carolina, USA).

RESULTS

Incidence of SNVCF After PVP for OVCF

Of the 661 consecutive patients who underwent PVP for OVCF between January 2011 and December 2013, 402 were enrolled in this study. Among the 402 patients included (338 women, 64 men), the age was 74.7 ± 8.5 years (range, 53–92 years). Follow-up was conducted for 4.4 ± 0.8 years (range, 4–7.1 years), during which SNVCF occurred in 120 patients (29.8% of the study sample), of whom 72 (17.9%) and 48 (11.9%) had AVCF and RVCF, respectively.

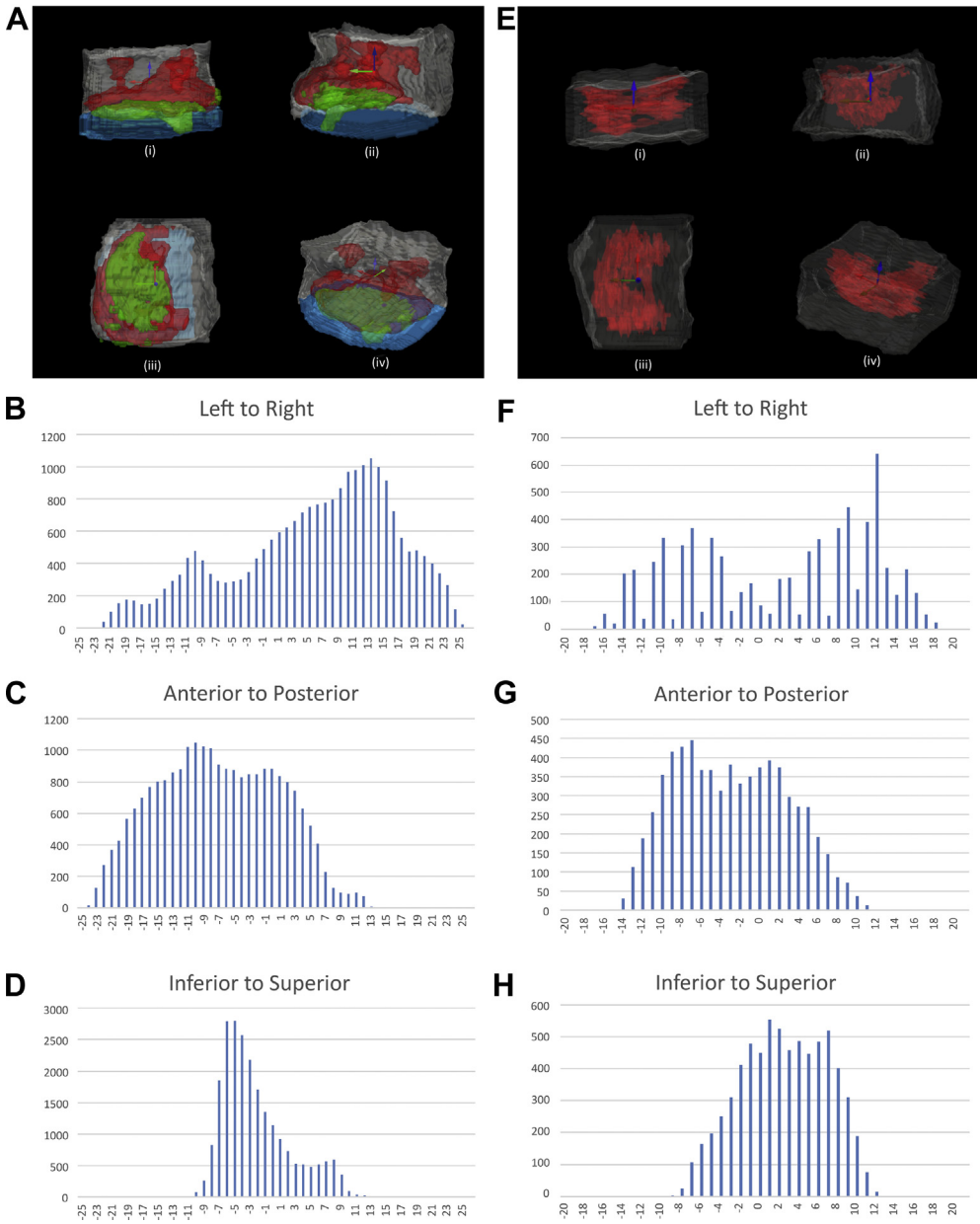

Figure 3. Visualization of bone cement voxel data in a representative case. (**A**) Three-dimensional visualization of the reconstructed model with its center and 3 axes (left-to-right axis, *red arrow*; posterior-to-anterior axis, *green arrow*; inferior-to-superior axis, *blue arrow*) of the local reference frame. Interactive three-dimensional results show minimal intradiscal bone cement leakage (*green*) into the inferior adjacent disc (*blue*) which is equivocal in two-dimensional images, as well as asymmetric distribution within the vertebral body. (**B**) Histogram showing even but right-skewed distribution of the cement along the left-to-right axis of the vertebra. (**C**) Histogram showing even but anteriorly skewed distribution of the cement along the posterior-to-anterior axis of the vertebra. (**D**) Histogram showing even but inferiorly skewed distribution of the cement along the inferior-to-superior axis. (**E**) Three-dimensional visualization of the reconstructed model with its center and 3 axes (left-to-right axis, *red arrow*; posterior-to-anterior axis, *green arrow*; inferior-to-superior axis, *blue arrow*) of the local reference frame. Interactive three-dimensional results show uneven and asymmetric distribution of the cement within the vertebral body. (**F**) Histogram showing uneven and right-skewed distribution of the cement along the left-to-right axis of the vertebra. (**G**) Histogram showing even but anteriorly skewed distribution of the cement along the posterior-to-anterior axis. (**H**) Histogram showing even but superiorly skewed (almost symmetric) distribution of the cement along the inferior-to-superior axis of the vertebra.

Relationship Between PVP-Treated OVCF and SNVCF

A total of 497 OVCFs were included in this study. Whereas single-level OVCF was noted in 323 patients, 2-level, 3-level, and 4-level OVCFs were observed in 62, 13, and 4 patients, respectively. Simple regression analysis showed that more OVCFs were associated with a higher risk of SNVCF after PVP, but this trend was not statistically significant ($P = 0.112$; Table 1).

Radiographic Parameters

The risk factors for AVCF, RVCF, and SNVCF were analyzed separately using data from patients with single-level OVCF (Table 2). The BMD was significantly lower in patients with SNVCF than in those without SNVCF (-3.9 ± 0.9 vs. -3.4 ± 0.8; $P < 0.001$, Wilcoxon rank-sum test; Table 2). The preoperative SI was significantly higher in patients with SNVCF than in those without SNVCF ($14.4° \pm 6.5°$ vs. $11.6° \pm 5.6°$; $P < 0.001$, Wilcoxon rank-sum test; Table 2). The incidence of intradiscal bone cement leakage was significantly higher in patients with AVCF than in those without new fractures or with non-AVCFs ($P = 0.001$, χ^2 test; Table 2).

PVP Procedure-Related Morphometric Parameters

Three-dimensional voxel-based analysis was performed using data pertaining to 182 patients who underwent postoperative CT or MRI. The risk factors for AVCF, RVCF, and SNVCF were analyzed separately using data from patients with single-level OVCF (Table 3). Based on the three-dimensional voxel-based analysis, the injected BCV was higher in the AVCF group than in the non-AVCF group (8001.5 ± 2824.1 vs. 5893.5 ± 2203.4 mm^3), but the difference was not statistically significant ($P = 0.122$). However, the BCV/VBV ratio was significantly higher in the AVCF group than in the non-AVCF group (0.3 ± 0.1 vs. 0.2 ± 0.1; $P < 0.001$, Wilcoxon rank-sum test; Table 3). The bone cement distribution along the inferior-to-superior axis differed significantly between the AVCF group and the non-AVCF group ($P = 0.027$, χ^2 test; Table 3).

Table 1. Risk for Secondary New Vertebral Compression Fracture According to the Number of Osteoporotic Vertebral Compression Fractures

	Simple Regression	Univariable Logistic Regression	
	P Value	Odds Ratio (95% Confidence Interval)	*P* Value
Number of osteoporotic vertebral compression fractures	0.112		
1		(reference)	
2		1.402 (0.790–2.489)	0.248
3		1.594 (0.508–4.999)	0.424
4		2.549 (0.354–18.367)	0.353

Values represent odds ratios and were calculated using logistic regression.

Risk Factors for SNVCF

On univariate analysis, only BMD, preoperative CR, preoperative SI, and intradiscal bone cement leakage showed significant association with SNVCF and AVCF ($P < 0.05$; Table 4). However, only BMD and SI showed significant association with RVCF ($P < 0.05$; Table 4). Among morphometric parameters, only the BCV/VBV ratio and bone cement distribution along the inferior-to-superior axis were significant risk factors of AVCF on univariate analysis ($P = 0.027$ and $P = 0.029$, respectively; Tables 3 and 4), whereas the injected BCV was not significantly associated with AVCF ($P = 0.591$). Univariate analysis also showed that the LIBCV/ADV ratio was not associated with AVCF even although intradiscal bone cement leakage was a significant risk factor for AVCF ($P = 0.169$ vs. $P = 0.045$; Table 4). On multivariate analysis, BMD was a statistically significant risk factor for SNVCF ($P = 0.041$), whereas bone cement leakage into the superior adjacent disc space was a statistically significant risk factor for AVCF ($P = 0.003$; Table 5). Thus, regarding SNVCF, the only risk factor supported by both univariate and multivariate analyses was BMD, confirming that low BMD is a strong risk factor for SNVCF ($P = 0.008$ and $P = 0.042$, respectively; Tables 4 and 5). Regarding AVCF, the only risk factor supported by both univariate and multivariate analyses was bone cement leakage into the superior adjacent disc space, confirming that this feature is a strong risk factor for AVCF ($P < 0.001$ and $P = 0.003$, respectively; Tables 4 and 5). Kaplan-Meier survival curves showed that AVCF occurred significantly more often and earlier than did RVCF, within the first 500 days after PVP, whereas the yearly incidence of RVCF remained constant throughout the follow-up period ($P = 0.011$).

DISCUSSION

SNVCF leads to severe back pain that cannot be easily controlled, often requiring subsequent PVP. Therefore, it is imperative to clarify the risk factors for SNVCF to obviate the possibility of this severe complication. SNVCF incidence is known to continue to increase over time, from 12% at 2 years to 52% at 4 years after PVP.[8,11] Therefore, it is necessary to consider data collected over a sufficiently long follow-up period, because short follow-up data might lead to biased conclusions. In this study, the overall incidence of SNVCFs was relatively high (29.8% during a minimum follow-up of 4 years, with an average follow-up of 5.2 years), which is believed to be caused by enrolling a large cohort and using long-term follow-up data, thus providing a more reliable estimate of the true incidence of SNVCFs after PVP for OVCF. Many studies have reported that the number of PVP-treated OVCFs was a risk factor for SNVCF,[13,17,18] suggesting that multiple-level PVP might be associated with a compromise of spinal posture, potentially leading to degenerative spinal diseases, including spinal deformities, which promote the recurrence of SNVCF.[13] Although this study did not show a statistically significant correlation between number of PVP-treated OVCF and SNVCFs, we believe that the number of PVP-treated OVCFs is a risk factor for SNVCF based on our clinical experience. Prospective studies with large cohorts and long-term follow-up periods are needed. Multiple previous studies have shown that low BMD is a crucial risk factor for SNVCF after PVP,[16,32,36] which is in agreement with our present results, confirming that low BMD is a strong risk factor for SNVCF. Immediate correction of osteoporosis

Table 2. Details Regarding the Incidence of Secondary New Vertebral Compression Fractures in Patients with Single-Level Osteoporotic Vertebral Compression Fracture

	SNVCF			AVCF			RVCF		
	Non-SNVCF (n = 232)	SNVCF (AVCF or RVCF) (n = 91)	*P* Value	Non-AVCF (Non-SNVCF or RVCF) (n = 277)	AVCF (n = 46)	*P* Value	Non-RVCF (Non-SNVCF or AVCF) (n = 278)	RVCF (n = 45)	*P* Value
Sex			0.868			0.708			0.553
Male	34 (14.7)	14 (15.4)		42 (15.2)	6 (13)		40 (14.4)	8 (17.8)	
Female	198 (85.3)	77 (84.6)		235 (84.8)	40 (87)		238 (85.6)	37 (82.2)	
Age (years)			0.105			0.106			0.736
	74.2 ± 9.1	75.9 ± 7.6		74.3 ± 8.9	76.7 ± 7.1		74.6 ± 8.8	75 ± 8.1	
Vertebroplasty technique			0.118			0.14			0.586
Unilateral extrapedicular	42 (18.1)	10 (11)		48 (17.3)	4 (8.7)		46 (16.6)	6 (13.3)	
Bilateral transpedicular	190 (81.9)	81 (89)		229 (82.7)	42 (91.3)		232 (83.5)	39 (86.7)	
Thoracolumbar junction fracture			0.102			0.734			**0.074**
No	104 (44.8)	50 (55)		131 (47.3)	23 (50)		127 (45.7)	27 (60)	
Yes	128 (55.2)	41 (45.1)		146 (52.7)	23 (50)		151 (54.3)	18 (40)	
Bone mineral density			**<0.001**			**0.005**			**0.006**
T score	−3.4 ± 0.8	−3.9 ± 0.9		−3.5 ± 0.8	−3.9 ± 0.8		−3.5 ± 0.8	−4 ± 1	
Preoperative kyphotic angle (°)			0.26			0.143			0.993
	−0.1 ± 8.4	0.4 ± 10.7		−0.1 ± 8.7	0.8 ± 11.7		0.1 ± 9	0.01 ± 9.8	
Preoperative sagittal index (°)			**<0.001**			**0.02***			**0.011***
	11.6 ± 5.6	14.4 ± 6.5		12.1 ± 5.9	14.4 ± 6.3		12.1 ± 5.8	14.5 ± 6.9	
Preoperative compression ratio			**0.003**			**0.012**			0.168
	20.5 ± 12.5	27 ± 15.8		21.4 ± 13.2	28 ± 16		21.7 ± 13.4	26 ± 15.7	
Body mass index (kg/m^2)			0.67*			0.954			0.353
	22.4 ± 3.3	22.2 ± 3.8		22.3 ± 3.4	22.5 ± 3.7		22.4 ± 3.4	21.9 ± 3.9	
Intradiscal bone cement leakage			**0.024**			**0.001**			0.521
None	148 (64.2)	44 (48.8)		177 (64.2)	15 (34.1)		165 (59.3)	28 (64.3)	
Inferior	23 (9.6)	9 (9.3)		26 (8.9)	6 (13.6)		28 (10.3)	3 (4.8)	
Superior	61 (26.2)	38 (41.9)		74 (26.9)	25 (52.3)		85 (30.4)	14 (31)	

The patients were stratified according to the incidence of SNVCFs.

Values are numbers (percentages) for categorical variables and mean ± standard deviation for continuous variables. *P*-values of <0.05 was considered to indicate statistical significance and are represented in bold.

P values are calculated using the *t* test* or Wilcoxon rank-sum test for continuous variables and the χ^2 test for categorical variables. *P* values are calculated using Wilcoxon rank-sum test for continuous variables and the χ^2 test for categorical variables.

SNVCF, secondary new vertebral compression fracture; AVCF, adjacent vertebral compression fracture; OVCF, osteoporotic vertebral compression fracture; RVCF, remote vertebral compression fracture.

Table 3. Detailed Statistics of the Three-Dimensional Voxel-Based Analysis

	SNVCF			AVCF			RVCF		
	Non-SNVCF (n = 91)	SNVCF (AVCF or RVCF) (n = 91)	*P* Value	Non-AVCF (Non-SNVCF or RVCF) (n = 136)	AVCF (n = 46)	*P* Value	Non-RVCF (Non-SNVCF or AVCF) (n = 137)	RVCF (n = 45)	*P* Value
Well distributed (spatially, evenly, and symmetrically)									
X-axis			0.657			0.306			0.606
No	47 (51.7)	44 (48.4)		71 (52.2)	20 (43.5)		67 (48.9)	24 (53.3)	
Yes	44 (48.4)	47 (51.7)		65 (47.8)	26 (56.5)		70 (51.1)	21 (46.7)	
Y-axis			>0.99			0.442			0.439
No	46 (50.6)	46 (50.6)		71 (52.2)	21 (45.7)		67 (48.9)	25 (55.6)	
Yes	45 (49.5)	45 (49.5)		65 (47.8)	25 (54.4)		70 (51.1)	20 (44.4)	
Z-axis			0.053			**0.027**			0.996
No	42 (46.2)	55 (60.4)		66 (48.5)	31 (67.4)		73 (53.3)	24 (53.3)	
Yes	49 (53.9)	36 (39.6)		70 (51.5)	15 (32.6)		64 (46.7)	21 (46.7)	
BCV (mm^3)			0.189			0.122			0.21
	5972.5 ± 3306.3	7995.5 ± 2646.1		5893.5 ± 2203.4	8001.5 ± 2824.1		6001.5 ± 5346.3	7886.2 ± 5364.1	
Ratio of BCV to vertebral body volume			0.065			**<0.001**			**0.007**
	0.2 ± 0.1	0.3 ± 0.1		0.2 ± 0.1	0.3 ± 0.1		0.2 ± 0.1	0.3 ± 0.1	
Leaked intradiscal BCV			0.546			0.648			0.212
Mean ± standard deviation (mm^3)	917.3 ± 1017.8	1230.2 ± 1613.6		767.4 ± 843.8	1660.4 ± 1913.2		1280.6 ± 1551.2	502.3 ± 241	
Median (interquartile range)	591.7 (357—1027.5)	470.6 (276.3—1585.6)		544.5 (347.9—919.8)	628.3 (187—2548.4)		591.7 (329.5—1451.8)	411 (326—599.7)	
Ratio of leaked intradiscal BCV to adjacent disc volume			0.209			0.466			0.057
	0.1 ± 0.1	0.1 ± 0.1		0.1 ± 0.1	0.1 ± 0.1		0.1 ± 0.1	0.04 ± 0.02	

The patients were stratified according to the incidence of SNVCFs.
Values are numbers (percentages) for categorical variables and mean ± standard deviation for continuous variables. *P*-values of <0.05 was considered to indicate statistical significance and are represented in bold.
P values are calculated using Wilcoxon rank-sum test for continuous variables and the χ^2 test for categorical variables.
AVCF, adjacent vertebral compression fracture; SNVCF, secondary new vertebral compression fracture; RVCF, remote vertebral compression fracture; BCV, bone cement volume.

Table 4. Univariate Logistic Regression Results for Risk Factors of Secondary New Vertebral Compression Fracture

	Non-SNVCF vs. SNVCF (AVCF or RVCF)		Non-AVCF (Non-SNVCF or RVCF) vs. AVCF		Non-RVCF (Non-SNVCF or AVCF) vs. RVCF	
Risk Factor	**Odds Ratio (95% CI)**	***P* Value**	**Odds Ratio (95% CI)**	***P* Value**	**Odds Ratio (95% CI)**	***P* Value**
Sex		0.868		0.709		0.554
Male						
Female	0.944 (0.481—1.856)		1.191 (0.475—2.986)		0.777 (0.337—1.790)	
Age	1.024 (0.994—1.054)	0.115	1.034 (0.995—1.075)	0.091	1.006 (0.970—1.044)	0.733
Vertebroplasty technique		0.121		0.149		0.587
Unilateral extrapedicular						
Bilateral transpedicular	1.791 (0.857—3.742)		2.201 (0.754—6.427)		1.289 (0.516—3.220)	
Thoracolumbar junction fracture		0.102		0.734		0.077
No						
Yes	0.666 (0.409—1.085)		0.897 (0.481—1.675)		0.561 (0.295—1.065)	
Bone mineral density	0.523 (0.390—0.701)	**<0.001**	0.628 (0.446—0.885)	**0.008**	0.583 (0.412—0.823)	**0.002**
Preoperative kyphotic angle	1.006 (0.980—1.034)	0.643	1.011 (0.976—1.048)	0.531	1 (0.966—1.035)	0.978
Preoperative sagittal index	1.084 (1.038—1.131)	**<0.001**	1.064 (1.009—1.121)	**0.021**	1.069 (1.014—1.127)	**0.013**
Preoperative compression ratio	1.034 (1.016—1.053)	**<0.001**	1.033 (1.011—1.056)	**0.003**	1.021 (0.999—1.044)	0.057
Body mass index	0.985 (0.918—1.057)	0.669	1.014 (0.926—1.11)	0.763	0.961 (0.877—1.053)	0.391
BCV	1.005 (0.970—1.030)	0.701	1.007 (0.963—1.052)	0.591	1 (0.932—1.084)	0.102
Ratio of BCV to vertebral body volume	1.019 (0.985—1.043)	0.057	1.052 (1.005—1.132)	**0.027**	1.023 (0.994—1.045)	0.075
Well-distributed cement (spatially, evenly, and symmetrically)						
Along the X-axis	1.141 (0.638—2.041)	0.657	1.42 (0.724—2.784)	0.307	0.838 (0.427—1.644)	0.606
Along the Y-axis	1 (0.559—1.788)	>0.99	1.3 (0.665—2.543)	0.443	0.766 (0.389—1.506)	0.439
Along the Z-axis	0.561 (0.311—1.011)	0.054	0.456 (0.226—0.921)	**0.029**	0.998 (0.508—1.96)	0.996
Bone cement leakage		0.358		0.083		0.577
No						
Yes	1.266 (0.766—2.093)		1.827 (0.925—3.610)		0.833 (0.437—1.586)	
Intradiscal bone cement leakage						
Inferior	1.273 (0.528—3.065)	0.591	2.9 (1.027—8.192)	**0.045**	0.429 (0.096—1.904)	0.266
Superior	2.1 (1.228—3.593)	**0.007**	3.655 (1.805—7.401)	**<0.001**	0.940 (0.461—1.916)	0.864
Leaked intradiscal BCV	1 (1—1)	0.41	1 (1—1.001)	**0.034**	0.999 (0.998—1)	0.135
Ratio of leaked intradiscal bone cement volume to adjacent disc volume	0.152 (<0.001—35.542)	0.495	52.216 (0.187—>999.999)	0.169	0.149 (<0.001—35.664)	0.325

The patients were stratified according to the incidence of SNVCFs. *P*-values of <0.05 was considered to indicate statistical significance and are represented in bold.
SNVCF, secondary new vertebral compression fracture; AVCF, adjacent vertebral compression fracture; RVCF, remote vertebral compression fracture; CI, confidence interval; BCV, bone cement volume.

after PVP is important for the prevention of SNVCFs. In a retrospective study of 60 patients, Kang et al.[19] reported that segmental KA was a significant risk factor for SNVCF after PVP, whereas another study found no significant correlation between KA and SNVCF.[13] In a retrospective study of 198 patients, Lee et al.[12] reported that segmental SI was not a significant risk factor for SNVCF after PVP. These discrepant results are likely related to differences in cohort size and follow-up periods. According to the present results obtained in a large cohort with long-term follow-up, SI was a strong risk factor for both AVCF and RVCF on univariate analysis. Our findings suggest that, because SI is obtained after subtracting the normal sagittal angle, the intensity of kyphotic

Table 5. Multivariate Logistic Regression Results for Risk Factors of Secondary New Vertebral Compression Fractures

	Model 1		Model 2		Model 3	
	Non-SNVCF vs. SNVCF (AVCF or RVCF)		Non-AVCF (Non-SNVCF or RVCF) vs. AVCF		Non-RVCF (Non-SNVCF or AVCF) vs. RVCF	
Risk Factor	**Odds Ratio (95% CI)**	***P* Value**	**Odds Ratio (95% CI)**	***P* Value**	**Odds Ratio (95% CI)**	***P* Value**
Bone mineral density	0.648 (0.426–0.985)	**0.042**			0.89 (0.401–1.976)	0.775
Preoperative sagittal index	1.063 (0.942–1.2)	0.319			1.06 (0.928–1.209)	0.391
Preoperative compression ratio	2.910 (0.125–67.578)	0.506				
Ratio of bone cement volume to vertebral body volume			1.11 (0.912–1.252)	0.402	1.012 (0.899–1.156)	0.823
Well-distributed cement*						
Along the Z-axis			0.391 (0.123–1.242)	0.111		
Intradiscal bone cement leakage						
Inferior			2.824 (0.882–9.04)	**0.08**		
Superior	2.423 (0.835–9.42)	**0.07**	3.354 (1.531–7.347)	**0.003**		

The patients were stratified according to the incidence of SNVCFs. *P*-values of <0.05 was considered to indicate statistical significance and are represented in bold.
SNVCF, secondary new vertebral compression fracture; AVCF, adjacent vertebral compression fracture; RVCF, remote vertebral compression fracture; CI, confidence interval.
*Cement distribution (spatially, evenly, and symmetrically).

change caused by OVCF may be more accurately reflected in SI than in KA (**Figure 1**). Regarding the injected BCV, there have been many studies that have described various methods. Whether the injected BCV is a risk factor for SNVCF remains controversial, and the optimal BCV has not been established.[26,36-41] Spinal biomechanical studies by Baroud et al. showed that rigid cement augmentation underneath the end plates acted as an upright pillar that severely reduced the inward bulging of the end plates of the augmented vertebra, resulting in increased stiffness of the intervertebral disc and increased inward bulging of the end plates of adjacent vertebra.[36,38] Another spinal biomechanical study by Baroud et al.[42] indicated that bone cement–augmented vertebral bodies become several times stiffer and several tens of times stronger than did untreated osteoporotic spinal cancellous bone, resulting in increased pressure on the intervertebral discs and untreated adjacent vertebral bodies. Baroud et al.[42] refer to this phenomenon as a "pillarlike" effect. A previous study by Li et al.[40] indicated that a larger BCV improves kyphosis but is positively correlated with SNVCF, which may be caused by changes in the biomechanics of the spinal segment.[13,40,43-45] Martinčič et al.[41] reported that the BCV should be $\geq$15% of the VBV to restore the stiffness of the fractured vertebral stiffness, whereas BCVs $>$20% increase the pressure on the adjacent vertebra rather than restoring the stiffness of the treated vertebral body. Some studies have reported conflicting results as to whether the injected BCV is a risk factor for SNVCF,[37] but these previous studies were conducted only in vitro or on cadavers. To our knowledge, all previous clinical studies on this topic obtained the injected BCV data from the medical records and not from accurate imaging documentation. To address these limitations, we conducted a clinical study using three-dimensional voxel-based morphometry, which facilitates more accurate measurements of BCVs and VBVs; moreover, we also analyzed the BCV/VBV ratio, because the biomechanical effect on the spinal column might be better reflected in the BCV/VBV ratio than in the absolute BCV. The approach used in the present study is the first of its kind in spinal surgery. There has been little research on the association between bone cement distribution and SNVCF after PVP.[28,29] Furthermore, although these previous studies have described the relationship of SNVCF with cement location and spatial distribution, the symmetry of cement distribution, which is important for biomechanical balance, has not been evaluated in this context.[13,28] In their study of the biomechanical effects of cement distribution, Liang et al.[28] did examine the symmetry of the cement distribution using a computer simulation technique, but they did not use clinical data. Another study on bone cement distribution in PVP used bone cement location data obtained by sectorizing the vertebral body region on two-dimensional images,[13] but this method was not elaborate and could not reflect the symmetry of the distribution within the vertebral body. In the present study, we performed three-dimensional voxel-based analysis, which enabled us to characterize the bone cement distribution according to both spatial and symmetry aspects. We found that bone cement distribution along the inferior-to-superior axis was a risk factor for AVCF according to the univariate analysis, suggesting that an uneven, rough, or skewed distribution of bone cement along the inferior-to-superior axis may increase the mechanical pressure on the adjacent vertebra. Many studies have reported that intradiscal bone cement leakage is a risk factor of AVCF after PVP.[16,23-25] In the present study, we also analyzed the relationship between AVCF and the LIBCV/ADV ratio, which may better reflect the biomechanical effect on adjacent vertebral bodies. However, according to the univariate analysis, the LIBCV/ADV ratio was not associated with AVCF, whereas intradiscal bone cement leakage and the BCV/VBV ratio were significant predictors of AVCF, suggesting that the

mechanical pressure on adjacent vertebral bodies is correlated not only with the intradiscal leakage itself but also with the relative filling of the fractured vertebral body (BCV/VBV ratio). Specifically, even if the LIBCV/ADV ratio is large, the mechanical pressure on the adjacent vertebral body may not increase if the injected BCV is small. Several in vitro biomechanical studies have suggested that vertebrae treated with PVP may increase the mechanical pressure on untreated adjacent vertebrae.[26,36,38,42,44] In their in vitro experimental study using cadaveric thoracic spinal segments, Kayanja et al.[44] found that the upper adjacent vertebra has increased anterior shear strain and is at greatest risk of AVCF. Our results are generally consistent with the results of those in vitro biomechanical studies. Relatively large volumes of bone cement and uneven or skewed distribution of the bone cement along the inferior-to-superior axis may create a pillarlike effect, leading to severely reduced inward bulge of the end plates of the augmented vertebra, which causes increased stiffness of the intervertebral disc and increased inward bulge of the end plates of the adjacent vertebra.[36,38] This pillarlike effect may be even more pronounced in patients with upper intradiscal bone cement leakage and low BMD.[42,44,46] For well-distributed bone cement along the inferior-superior axis and for avoiding intradiscal bone cement leakage, proper needle placement is needed, and venography and adjustment of bone cement viscosity are recommended.[47-49] The present study has several limitations associated mainly with the retrospective nature of the analysis. Postoperative CT and MRI were not routinely performed; thus, data of only 182 of the 323 patients with single-level OVCF were used in the voxel-based analyses. The inconsistency in timing of performing postoperative CTs and MRIs and the fact that not all patients had imaging are limitations that may be sources of bias. Furthermore, although the three-dimensional voxel-based analyses were performed using the same protocol, there was a difference in the size of unit-voxel because resolution of the MRI was low; this may be a source of bias. A randomized controlled prospective study using three-dimensional voxel-based analysis based on CT scans is required to confirm our present findings.

CONCLUSIONS

Low BMD, high preoperative SI, and high preoperative CR may be predictive factors for SNVCFs after PVP. As preventive strategies in patients with these predictive factors, the bone cement should be injected so that it becomes evenly and symmetrically distributed along the inferior-to-superior axis during PVP; moreover, the injected BCV should not be excessively large, especially to prevent AVCF. Care should be taken to inject the bone cement without leakage into the adjacent disc space, especially into the superior adjacent disc space. Careful follow-up of the BMD and immediate correction of osteoporosis after PVP are crucial for preventing SNVCF.

REFERENCES

1. Buchbinder R, Osborne RH, Ebeling PR, et al. A randomized trial of vertebroplasty for painful osteoporotic vertebral fractures. *N Engl J Med*. 2009;361:557-568.

2. Kallmes DF, Comstock BA, Heagerty PJ, et al. A randomized trial of vertebroplasty for osteoporotic spinal fractures. *N Engl J Med*. 2009;361:569-579.

3. Rousing R, Hansen KL, Andersen MO, Jespersen SM, Thomsen K, Lauritsen JM. Twelve-months follow-up in forty-nine patients with acute/semiacute osteoporotic vertebral fractures treated conservatively or with percutaneous vertebroplasty. *Spine*. 2010;35:478-482.

4. Clark W, Bird P, Gonski P, et al. Safety and efficacy of vertebroplasty for acute painful osteoporotic fractures (VAPOUR): a multicentre, randomised, double-blind, placebo-controlled trial. *Lancet*. 2016;388:1408-1416.

5. Yang EZ, Xu JG, Huang GZ, et al. Percutaneous vertebroplasty versus conservative treatment in aged patients with acute osteoporotic vertebral compression fractures: a prospective randomized controlled clinical study. *Spine*. 2016;41:653-660.

6. Jang JS, Lee SH, Jung SK. Pulmonary embolism of polymethylmethacrylate after percutaneous vertebroplasty. *Spine*. 2002;27:416-418.

7. Moreland DB, Landi MK, Grand W. Vertebroplasty: techniques to avoid complications. *Spine J*. 2001;1:66-71.

8. Grados F, Depriester C, Cayrolle G, Hardy N, Deramond H, Fardellone P. Long-term observations of vertebral osteoporotic fractures treated by percutaneous vertebroplasty. *Rheumatology (Oxford)*. 2000;39:1410-1414.

9. Trout AT, Kallmes DF, Kaufmann TJ. New fractures after vertebroplasty: adjacent fractures occur significantly sooner. *AJNR Am J Neuroradiol*. 2006;27:217-223.

10. Tseng YY, Yang TC, Tu PH, Lo YL, Yang ST. Repeated and multiple new vertebral compression fractures after percutaneous transpedicular vertebroplasty. *Spine*. 2009;34:1917-1922.

11. Uppin AA, Hirsch JA, Centenera LV, Pfiefer BA, Pazianos AG, Choi IS. Occurrence of new vertebral body fracture after percutaneous vertebroplasty in patients with osteoporosis. *Radiology*. 2003;226:119-124.

12. Lee DG, Park CK, Park CJ, Lee DC, Hwang JH. Analysis of risk factors causing new symptomatic vertebral compression fractures after percutaneous vertebroplasty for painful osteoporotic vertebral compression fractures: a 4-year follow-up. *J Spinal Disord Tech*. 2015;28:578-583.

13. Bae JS, Park JH, Kim KJ, Kim HS, Jang IT. Analysis of risk factors for secondary new vertebral compression fracture following percutaneous vertebroplasty in patients with osteoporosis. *World Neurosurg*. 2017;99:387-394.

14. Belkoff SM, Mathis JM, Jasper LE, Deramond H. The biomechanics of vertebroplasty. The effect of cement volume on mechanical behavior. *Spine*. 2001;26:1537-1541.

15. Hey HW, Tan JH, Tan CS, Tan HM, Lau PH, Hee HT. Subsequent vertebral fractures post cement augmentation of the thoracolumbar spine: does it correlate with level-specific bone mineral density scores? *Spine*. 2015;40:1903-1909.

16. Zhang Z, Fan J, Ding Q, Wu M, Yin G. Risk factors for new osteoporotic vertebral compression fractures after vertebroplasty: a systematic review and meta-analysis. *J Spinal Disord Tech*. 2013;26:150-157.

17. Voormolen MH, Lohle PN, Juttmann JR, van der Graaf Y, Fransen H, Lampmann LE. The risk of new osteoporotic vertebral compression fractures in the year after percutaneous vertebroplasty. *J Vasc Interv Radiol*. 2006;17:71-76.

18. Yokoyama K, Kawanishi M, Yamada M, et al. Safety and therapeutic efficacy of the second treatment for new fractures developed after initial vertebroplasty performed for painful vertebral compression fractures. *Neurol Res*. 2013;35:608-613.

19. Kang SK, Lee CW, Park NK, et al. Predictive risk factors for refracture after percutaneous vertebroplasty. *Ann Rehabil Med*. 2011;35:844-851.

20. Lu J, Jiang G, Lu B, Shi C, Luo K, Yue B. The positive correlation between upper adjacent vertebral fracture and the kyphosis angle of injured vertebral body after percutaneous kyphoplasty: an in vitro study. *Clin Neurol Neurosurg*. 2015;139:272-277.

21. Farcy JP, Weidenbaum M, Glassman SD. Sagittal index in management of thoracolumbar burst fractures. *Spine*. 1990;15:958-965.

22. Lin CC, Chen IH, Yu TC, Chin IH, Chung HW. New symptomatic compression fracture after

percutaneous vertebroplasty at the thoracolumbar junction. *AJNR Am J Neuroradiol*. 2007;28:1042-1045.

23. Chen X, Ren J, Zhang J, Li S, Liu Z. Impact of cement placement and leakage in osteoporotic vertebral compression fractures followed by percutaneous vertebroplasty. *Clin Spine Surg*. 2016; 29:365-370.

24. Jesse MK, Petersen B, Glueck D, Kriedler S. Effect of the location of endplate cement extravasation on adjacent level fracture in osteoporotic patients undergoing vertebroplasty and kyphoplasty. *Pain Physician*. 2015;18:805-814.

25. Lin EP, Ekholm S, Hiwatashi A, Westesson PL. Vertebroplasty: cement leakage into the disc increases the risk of new fracture of adjacent vertebral body. *AJNR Am J Neuroradiol*. 2004;25:175-180.

26. Belkoff SM, Mathis JM, Erbe EM, Fenton DC. Biomechanical evaluation of a new bone cement for use in vertebroplasty. *Spine*. 2000;25:1061-1064.

27. Kolb JP, Kueny RA, Püschel K, et al. Does the cement stiffness affect fatigue fracture strength of vertebrae after cement augmentation in osteoporotic patients? *Eur Spine J*. 2013;22:1650-1656.

28. Liang D, Ye LQ, Jiang XB, et al. Biomechanical effects of cement distribution in the fractured area on osteoporotic vertebral compression fractures: a three-dimensional finite element analysis. *J Surg Res*. 2015;195:246-256.

29. Tanigawa N, Komemushi A, Kariya S, et al. Relationship between cement distribution pattern and new compression fracture after percutaneous vertebroplasty. *AJR Am J Roentgenol*. 2007;189: 348-352.

30. Woermann FG, Free SL, Koepp MJ, Sisodiya SM, Duncan JS. Abnormal cerebral structure in juvenile myoclonic epilepsy demonstrated with voxel-based analysis of MRI. *Brain*. 1999;122:2101-2108.

31. Yamasue H, Kasai K, Iwanami A, et al. Voxel-based analysis of MRI reveals anterior cingulate gray-matter volume reduction in posttraumatic stress disorder due to terrorism. *Proc Natl Acad Sci U S A*. 2003;22:9039-9043.

32. Lee SW, Hong JT, Son BC, Sung JH, Kim IS, Park CK. Analysis of accuracy of kyphotic angle measurement for vertebral osteoporotic compression fractures. *J Clin Neurosci*. 2007;14:961-965.

33. Singh R, Kumar RR, Setia N, Magu S. A prospective study of neurological outcome in relation to findings of imaging modalities in acute spinal cord injury. *Asian J Neurosurg*. 2015;10: 181-189.

34. Lemieux L, Jagoe R, Fish DR, Kitchen ND, Thomas DG. A patient-to-computed-tomography image registration method based on digitally reconstructed radiographs. *Med Phys*. 1994;21: 1749-1760.

35. Enkhbaatar N-E, Inoue S, Yamamuro H, et al. MR imaging with apparent diffusion coefficient histogram analysis in rectal cancer. *Radiology*. 2018; 288:129-137.

36. Baroud G, Nemes J, Heini P, Steffen T. Load shift of the intervertebral disc after a vertebroplasty: a finite-element study. *Eur Spine J*. 2003;12:421-426.

37. Aquarius R, Van der Zijden AM, Homminga J, Verdonschot N, Tanck E. Does bone cement in percutaneous vertebroplasty act as a stress riser? *Spine*. 2013;38:2092-2097.

38. Baroud G, Heini P, Nemes J, Bohner M, Ferguson S, Steffen T. Biomechanical explanation of adjacent fractures following vertebroplasty. *Radiology*. 2003;229:606-607.

39. Graham J, Ahn C, Hai N, Buch BD. Effect of bone density on vertebral strength and stiffness after percutaneous vertebroplasty. *Spine*. 2007;32: 505-511.

40. Li YA, Lin CL, Chang MC, Liu CL, Chen TH, Lai SC. Subsequent vertebral fracture after vertebroplasty: incidence and analysis of risk factors. *Spine*. 2012;37:179-183.

41. Martinčič D, Brojan M, Kosel F, et al. Minimum cement volume for vertebroplasty. *Int Orthop*. 2015; 39:727-733.

42. Baroud G, Vant C, Wilcox R. Long-term effects of vertebroplasty: adjacent vertebral fractures. *J Long Term Eff Med Implants*. 2006;16:265-280.

43. Eichler MC, Spross C, Ewers A, Mayer R, Külling FA. Prophylactic adjacent-segment vertebroplasty following kyphoplasty for a single osteoporotic vertebral fracture and the risk of adjacent fractures: a retrospective study and clinical experience. *J Neurosurg Spine*. 2016;25:528-534.

44. Kayanja MM, Ferrara LA, Lieberman IH. Distribution of anterior cortical shear strain after a thoracic wedge compression fracture. *Spine J*. 2004;4:76-87.

45. Luo J, Annesley-Williams DJ, Adams MA, Dolan P. How are adjacent spinal levels affected by vertebral fracture and by vertebroplasty? A biomechanical study on cadaveric spines. *Spine J*. 2017; 17:863-874.

46. Syed MI, Patel NA, Jan S, Harron MS, Morar K, Shaikh A. Intradiskal extravasation with low-volume cement filling in percutaneous vertebroplasty. *AJNR Am J Neuroradiol*. 2005;26: 2397-2401.

47. Ringer AJ, Bhamidipaty SV. Percutaneous access to the vertebral bodies: a video and fluoroscopic overview of access techniques for trans-, extra-, and infrapedicular approaches. *World Neurosurg*. 2013;80:428-435.

48. Tanigawa N, Komemushi A, Kariya S, Kojima H, Sawada S. Intraosseous venography with carbon dioxide contrast agent in percutaneous vertebroplasty. *AJR Am J Roentgenol*. 2005;184:567-570.

49. Xin L, Bungartz M, Maenz S, et al. Decreased extrusion of calcium phosphate cement versus high viscosity PMMA cement into spongious bone marrow-an ex vivo and in vivo study in sheep vertebrae. *Spine J*. 2016;16:1468-1477.

Conflict of interest statement: This study was supported by research grants from Hanmi Pharmaceutical Co. Ltd. (HM-IIT-ESO-039).

Received 7 November 2018; accepted 8 January 2019

Citation: World Neurosurg. (2019) 125:e146-e157.
https://doi.org/10.1016/j.wneu.2019.01.020

Journal homepage: ***www.journals.elsevier.com/world-neurosurgery***

Available online: ***www.sciencedirect.com***